

Ventricular assist device implantation improves skeletal muscle function, oxidative capacity, and growth hormone/insulin-like growth factor-1 axis signaling in patients with advanced heart failure

Tuba Khawaja · Aalab Chokshi · Ruiping Ji · Tomoko S. Kato · Katherine Xu ·
Cynthia Zizola · Christina Wu · Daniel E. Forman · Takeyoshi Ota · Peter Kennel ·
Hiroo Takayama · Yoshifumi Naka · Isaac George · Donna Mancini · Christian P. Schulze

Received: 17 April 2014 / Accepted: 9 July 2014 / Published online: 7 August 2014
© Springer-Verlag Berlin Heidelberg 2014

Abstract

Background Skeletal muscle dysfunction in patients with heart failure (HF) has been linked to impaired growth hormone (GH)/insulin-like growth factor (IGF)-1 signaling. We hypothesized that ventricular assist device (VAD) implantation reverses GH/IGF-1 axis dysfunction and improves muscle metabolism in HF.

Methods Blood and rectus abdominis muscle samples were collected during VAD implantation and explantation from patients with HF and controls. Clinical data were obtained from medical records, biomarkers measured by enzyme-linked immunosorbent assay (ELISA), and gene expression analyzed by reverse transcription and real-time polymerase chain reaction (RT-PCR). Grip strength was assessed by dynamometry. Oxidative capacity was measured using oleate oxidation rates. Muscle fiber type and size were assessed by histology.

Results Elevated GH (0.27 ± 0.27 versus 3.6 ± 7.7 ng/ml in HF; $p=0.0002$) and lower IGF-1 and insulin-like growth factor binding protein (IGFBP)-3 were found in HF (IGF-1,

144 ± 41 versus 74 ± 45 ng/ml in HF, $p < 0.05$; and IGFBP-3, $3,880 \pm 934$ versus $1,935 \pm 862$ ng/ml in HF, $p = 0.05$). The GH/IGF-1 ratio, a marker of GH resistance, was elevated in HF (0.002 ± 0.002 versus 0.048 ± 0.1 pre-VAD; $p < 0.0039$). After VAD support, skeletal muscle expression of IGF-1 and IGFBP-3 increased (10-fold and 5-fold, respectively; $p < 0.05$) accompanied by enhanced oxidative gene expression (CD36, CPT1, and PGC1 α) and increased oxidation rates ($+1.37$ -fold; $p < 0.05$). Further, VAD implantation increased the oxidative muscle fiber proportion (38 versus 54 %, $p = 0.031$), fiber cross-sectional area (CSA) ($1,005 \pm 668$ versus $1,240 \pm 670$ μm^2 , $p < 0.001$), and Akt phosphorylation state in skeletal muscle. Finally, hand grip strength increased 26.5 ± 27.5 % at 180 days on-VAD ($p < 0.05$ versus baseline).

Conclusion Our data demonstrate that VAD implantation corrects GH/IGF-1 signaling, improves muscle structure and function, and enhances oxidative muscle metabolism in patients with advanced HF.

Keywords Skeletal muscle · Heart failure · Cardiovascular surgery · Metabolism · Growth factors

T. Khawaja · A. Chokshi · R. Ji · T. S. Kato · K. Xu · C. Zizola ·
C. Wu · D. E. Forman · P. Kennel · H. Takayama · Y. Naka ·
I. George · D. Mancini · C. P. Schulze (✉)
Center for Advanced Cardiac Care, Department of Medicine,
Division of Cardiology, Columbia University Medical Center, 622
West 168th Street, PH 10, Room 203, New York, NY 10032, USA
e-mail: pcs2121@cumc.columbia.edu

T. Ota · H. Takayama · Y. Naka · I. George
Department of Surgery, Division of Cardiothoracic Surgery,
Columbia University Medical Center, New York, NY, USA

D. E. Forman
Cardiovascular Division, Department of Medicine, Brigham and
Women's Hospital, Harvard Medical School, Boston, MA, USA

Metabolic abnormalities develop in patients with advanced heart failure (HF) and impact every organ system [1–3]. End-stage HF is associated with a catabolic state that affects both systemic and local metabolism, leading to a negative protein balance driven by increased energy expenditure. Skeletal muscle, the largest reservoir of protein, is prone to wasting in catabolic states including HF. Exercise intolerance, a clinical hallmark of patients with HF, is determined not only by impaired central hemodynamics but also by peripheral abnormalities in skeletal muscle metabolism, structure, and function

[4–6]. These intrinsic skeletal muscle changes have been linked to endocrine and paracrine abnormalities [1], increased oxidative stress [7], impaired intramuscular Ca^{2+} handling [8], and reduced capillary density [9].

A major anabolic system of the human body is the growth hormone (GH)/insulin-like-growth factor (IGF)-1 signaling axis with well-established effects on muscle mass and function and in the regulation of lipolysis and lipid oxidation [10]. Growth hormone resistance with inappropriately low levels of IGF-1 develops in chronic inflammatory states and is associated with catabolic syndromes including advanced HF [11, 12]. Growth hormone resistance has been linked to inflammation tumor necrosis factor- α - and interleukin-6-mediated inhibition of hepatic GH signaling as well as levels of angiotensin II [13].

Therapeutic interventions to address progressive catabolism in advanced HF are limited. Interventions known to increase circulating IGF-1 levels and increase muscle mass in HF are GH supplementation and aerobic exercise training [14, 15], and GH resistance resolves following cardiac transplantation [16]. Improvements in systemic and local metabolism have also been linked to corrected hemodynamics and tissue perfusion following the implantation of ventricular assist devices in patients with advanced HF both as destination therapy and as bridge-to-transplantation [17, 18]. Multiple studies have shown that ventricular assist device (VAD) implantation not only provides adequate hemodynamic support but is also effective in rehabilitating patients based on improved renal and hepatic function as well as physical capacity assessments [19–22]. We, therefore, hypothesized that implantation of a VAD would improve skeletal muscle function and metabolism and reverse GH/IGF-1 axis dysfunction in patients with HF.

1 Methods

1.1 Study design

We analyzed a cohort of 31 patients with advanced HF undergoing VAD implantation ($n=25$) and explantation ($n=25$). Data from 19 patients were available both at the time of VAD implantation and explantation for paired analyses. All patients underwent continuous flow VAD implantation (Heartmate II, Thoratec Inc.) at Columbia University Medical Center between August 2010 and April 2012. Controls ($n=10$) were recruited among healthy volunteers at our institution. Controls were excluded if they had evidence of diabetes, inflammatory diseases, hyperlipidemia, renal dysfunction, or liver dysfunction. We collected standard clinical information, medical history, clinical laboratory data, and echocardiographic data for all patients and control subjects from electronic medical records or through direct analysis.

The study was approved by the Institutional Review Board of Columbia University, and all patients provided written informed consent before inclusion into the study.

1.2 Sample collection

Fasting blood samples were collected from all study subjects (31 patients with HF and 10 controls). Paired serum samples (pre-VAD and post-VAD) were available from 19 patients. Rectus abdominis muscle samples were collected during surgical VAD implantation and at explantation during cardiac transplantation from 12 non-paired patients.

1.3 Grip strength analysis

Grip strength was measured with a hand dynamometer (Jamar, Inc.) in a subgroup of 15 patients at baseline and at various time points up to 180 days following VAD implantation. While resting the elbows on the hips, the patients were asked to squeeze the dynamometer at maximum force (three repetitions 10 s apart for both dominant and non-dominant hands). Values from the dominant and non-dominant arm were averaged and normalized for body weight to exclude weight-related differences. Dynamics are reported as percent changes from baseline.

1.4 Serum analysis

Samples were centrifuged at $10,000\times g$ and stored at $-80\text{ }^{\circ}\text{C}$ until analysis. Serum samples were analyzed using enzyme-linked immunosorbent assays (ELISAs) to measure the serum levels of GH, IGF-1, and insulin-like growth factor binding protein (IGFBP)-3 (Quantikine, R&D Systems, Minneapolis, MN, USA).

1.5 Gene expression analysis

Total RNA was extracted from rectus abdominis muscle samples ($n=10$) using the phenol-chloroform RNA extraction method. RNA was then used to prepare complementary DNA (cDNA) with the Superscript reverse transcriptase cDNA kit (Invitrogen), and the abundance of the specific mRNAs was determined by reverse transcription and real-time polymerase chain reaction (RT-PCR) (Bio-RAD) using previously described primers (IGF-1, IGFBP3, IGF receptor, CD36, CPT1, GLUT4, PDK4, PGC1 α) [23]. Gene expression was normalized using expression of beta-actin and expressed as relative expression.

1.6 Histological analysis

Muscle fiber cross-sectional area (CSA) and capillary density were analyzed in a subset of six patients before and after VAD implantation using previously described methods [24]. In

short, H&E-stained sections (5 μm) of rectus abdominis muscle samples were reviewed microscopically at $\times 10$ magnification (Nikon Eclipse E 200) and on three independent images per slide, fiber size and capillaries were analyzed using standard image-processing software (NIH ImageJ). Capillaries were detected by immunohistochemistry using specific antibodies for detection of E-selectin (Santa Cruz, Inc.). Capillaries were counted on each image and expressed as number of capillaries per muscle fiber. Muscle fibers were only measured if their shape was not elongated to an ellipsoid shape which would imply a sectioning not perpendicular to the long axis. For all slides, the scale was set to 2.84 pixels/unit based on a standardized stage micrometer for $\times 10$ magnification. Frequency histograms were constructed based on the number of muscle fibers falling within CSA groups.

Immunohistochemistry was performed for the characterization of muscle fiber oxidative quality and fiber typing. Paraffin-embedded sections (5 μm) were first incubated in 5 % goat serum to reduce non-specific immunoreactivity and subsequently with primary anti-myosin antibodies (monoclonal anti-fast twitch skeletal muscle myosin, Sigma, 1:400). Specific immunoreactivity was detected with a secondary rabbit anti-mouse antibody (Pierce, 1:400) followed by conjugation with avidin-biotin-complex (ABC Kit, Pierce). Immunopositive fibers were quantified and expressed as percent of all muscle fibers.

1.7 Fatty acid oxidation analysis

Fatty acid oxidation in muscle tissues was performed in rectus abdominis muscle samples obtained from patients before and after VAD implantation ($n=6$ per group) by measuring the production of [^{14}C] CO_2 from [^{14}C] oleic acid (PerkinElmer, Waltham, MA). Approximately 20–30 mg of muscle tissues was transferred into 10-mL Kontes® flasks (Sigma-Aldrich, St. Louis, MO) containing 1 mL of modified Krebs Ringer's solution (115 mM NaCl, 2.5 mM KCl, 1.2 mM KH_2PO_4 , 10 mM NaHCO_3 , 10 mM HEPES) with 1.5 % BSA, 0.2 mM oleic acid, 2 $\mu\text{Ci}/\text{mL}$ [^{14}C] oleic acid, and 1 mM glucose. The flasks were immediately cupped with rubber stoppers containing an attached central well with a 3×3 cm filter paper soaked in 300 μL KOH. After 1 h of incubation at 37 $^\circ\text{C}$, 200 μL of 70 % perchloric acid was injected into the flask. The flasks were incubated for an additional 1 h at 37 $^\circ\text{C}$ with shaking at 70 Hz. The filter papers containing the trapped [^{14}C] CO_2 were transferred to liquid scintillation tubes and assessed for radioactivity in a liquid scintillation counter.

1.8 Statistical analysis

Data are presented as mean \pm standard deviation or as proportion (percent). Normality was tested using the Kolmogorov-Smirnov test. Group comparisons were made using the χ^2 or

Fisher's exact test for categorical variables and the Student's *t* test or one-way analysis of variance with Tukey's post hoc testing for continuous variables. For variables that did not follow a Gaussian distribution, the Mann-Whitney *U* test or Kruskal-Wallis analysis of variance was used. Strength of association between variables was assessed by either Pearson or Spearman correlation, as appropriate. Data were analyzed using GraphPad Prism 5.0 (La Jolla, CA). A *p* value <0.05 was considered statistically significant.

2 Results

2.1 Baseline demographics

Clinical characteristics of all patients are summarized in Table 1. Five patients (20 %) had a history of dilated cardiomyopathy, 15 patients (60 %) had a history of ischemic cardiomyopathy, and 5 (20 %) had other causes of HF. Controls did not have any cardiac disease and did not report a history of smoking or hypertension. The mean duration of VAD support was 358 ± 294 days. BMI did not change significantly during the time of VAD support. Laboratory values in patients with advanced HF before and after VAD placement and controls are summarized in Table 2.

2.2 Serum markers of the GH/IGF-1 axis

The serum markers for the GH/IGF-1 axis were analyzed in all subjects (Fig. 1). Serum levels of GH were higher in patients with advanced HF (pre-VAD) compared to controls (0.27 ± 0.27 versus 3.6 ± 7.7 ng/ml in advanced HF pre-VAD; $p=0.0002$) while IGF-1 and IGFBP both were lower in HF (IGF-1, 144 ± 41 versus 74 ± 45 ng/ml in advanced HF pre-VAD, $p<0.05$; and IGFBP-3, $3,880\pm 934$ versus $1,935\pm 862$ ng/ml in advanced HF pre-VAD, $p=0.05$). No changes were found in IGF-1 or IGFBP3 serum levels after VAD implantation. Circulating levels of GH decreased to 1.77 ± 2.9 ng/ml following VAD implantation ($p=\text{NS}$ versus pre-VAD). The GH/IGF-1 ratio, a marker of GH resistance, was elevated in patients with advanced HF compared to controls (0.002 ± 0.002 in controls versus 0.048 ± 0.1 pre-VAD; $p<0.0039$) and decreased numerically during VAD support (0.032 ± 0.065 ; $p=0.2$ versus pre-VAD). No relation was found between duration of device support and changes in systemic or local GH/IGF-1 axis parameters (coefficients of correlation: duration of left ventricular assist device (LVAD) support vs. GH changes $R^2=0.0031$, duration of LVAD support vs. IGF1 changes $R^2=0.1925$, duration of LVAD vs. GH/IGF-ratio $R^2=0.0149$; all $p=\text{NS}$).

Table 1 Baseline demographics

	Controls (<i>n</i> =10)	VAD implant (<i>n</i> =25)	VAD explant (<i>n</i> =25)
Age at VAD implantation (years)	62±7	64±7	62±8
Gender (% male)	9 (90)	22 (88)	21 (84)
BMI (kg/m ²)	25.2±2.9	26.8±4.3	25.6±3.5
Etiology of HF			
DCM		5 (20)	
ICM		15 (60)	
Other		5 (20)	
Treatment (no. of patients, %)			
Diuretics	–	18 (72)	16 (64)
β-blockers	–	16 (64)	20 (80)
ACE inhibitors/AII antagonists	–	12 (48)	12 (48)
Coumadin	–	9 (36)	13 (52)

2.3 Hand grip strength measurements

Measurement of hand grip strength normalized for body weight was performed in patients with advanced HF before undergoing VAD implantation and in controls. Further, handgrip strength was measured at various time points after the VAD implantation. The readings were taken for both the dominant and non-dominant hands and averaged. Patients with advanced HF had lower handgrip strength corrected for body weight prior to VAD implantation (35.8±7.8 versus 55.6±12.7 in controls; *p*=0.001). There was a relative increase in the average handgrip strength normalized for BW over time reaching >25 % after 6 months on-VAD support (2 months +12.8±20.7 %, 4 months +18.9±21.4 %, and 6 months +26.5±27.5 % of baseline pre-VAD; *p*<0.05 versus baseline) (Fig. 2).

Table 2 Dynamics of laboratory values during VAD support

	Control (<i>n</i> =10)	VAD implant (<i>n</i> =25)	VAD explant (<i>n</i> =25)
White blood cell count (×10 ³ /μL)	5.1±0.3	8.7±3.5	8.5±4.1
Hematocrit (%)	40.2±5.7	28.2±10.2*	31.7±4.6
Platelets (×10 ³ /μL)	217±17	203±85	178±73
Sodium (mEq/L)	140±12	135±4	138±4
Blood urea nitrogen (mg/dL)	18±4	33±16*	25±11
Creatinine (mg/dL)	1.0±0.2	2.5±5.3	1.3±0.6
Albumin (mg/dL)	4.7±0.4	3.5±0.5*	3.7±0.5 [†]
Total bilirubin (mg/dL)	0.6±0.2	1.6±1.8	1.1±0.9
Direct bilirubin (mg/dL)	0.1±0.0	0.6±1.0	0.5±0.5
Aspartate aminotransferase (U/L)	25±10	36±27	56±56
Alanine transaminase (U/L)	25±7	29±25	25±22
Alkaline phosphatase (U/L)	72±15	89±36	76±30

**p*<0.05 between implants and controls; [†]*p*<0.05 between explants and controls

2.4 Analysis of skeletal muscle gene expression following VAD implantation

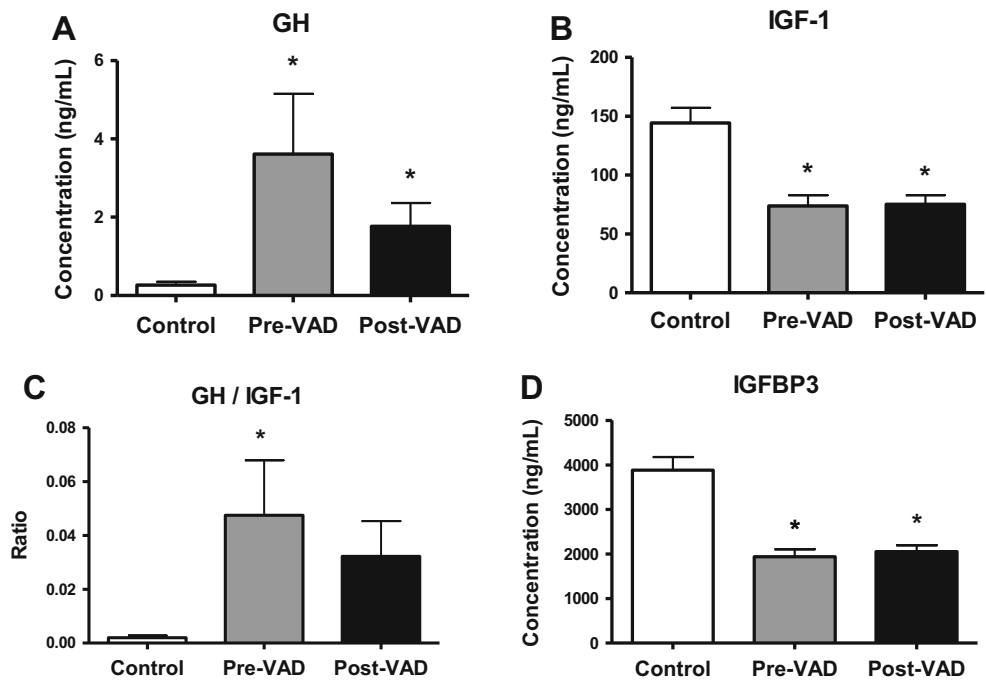
The local skeletal muscle expression of anabolic IGF-1 increased 15-fold (*p*=0.047), and expression of IGF binding protein (BP)-3 demonstrated a trend towards an increase (*p*=0.06) in response to hemodynamic improvement by VAD implantation. Expression of the IGF receptor in skeletal muscle decreased following VAD implantation (*p*=0.048) (Fig. 3a).

We next analyzed the expression of marker genes of glucose and fatty acid metabolism. The expression of the insulin-dependent glucose transporter type 4 (GLUT4) increased in muscle samples (+6.7-fold versus pre-VAD, *p*=0.046) implicating increased glucose transport capacity following VAD implantation. Pyruvate dehydrogenase kinase-4 (PDK-4) decreased by 50 % during VAD support (*p*=NS). Of note, skeletal muscle expression levels of the scavenger receptor, cluster of differentiation (CD) 36, and the mitochondrial fatty acid uptake transporter, carnitine palmitoyl transferase (CPT)-1, both genes indicative of fatty acid oxidative metabolism, increased significantly (CD36, +3-fold and CPT1, +3.5-fold, both *p*<0.05 versus pre-VAD). Finally, expression levels of peroxisome proliferator-activated receptor γ co-activator-1α (PGC1α), a master regulator of oxidative metabolism, increased 3.2-fold following VAD implantation in rectus abdominis muscle of patients with advanced HF (*p*=0.03 versus pre-VAD; Fig. 3b).

2.5 Analysis of skeletal muscle histology and oxidative capacity

Histological analysis of skeletal muscle specimens obtained from patients before and after VAD implantation revealed an increase in muscle fiber cross-sectional area following VAD implantation (mean CSA, 1,005±668 versus 1,240±670 μm²,

Fig. 1 Serum markers of the GH/IGF-1 axis in patients with advanced HF before and after VAD implantation and controls. **a** Levels of GH in HF were higher compared to controls and remained elevated after VAD implantation. **b** Suppression of circulating IGF-1 in advanced HF compared to controls without changes following VAD implantation. **c** Changes in the GH/IGF-1 ratio showed improved GH sensitivity following VAD placement. **d** IGFBP3 was lower in advanced HF compared to controls with or without changes following VAD placement (* $p < 0.05$ versus controls, # $p < 0.05$ versus pre-VAD; 10 controls, 25 patients pre-VAD and post-VAD for all measures)



$p < 0.001$) (Fig. 4a). A frequency histogram of fiber cross-sectional area shows a distinct right shift in the percentage of fibers with greater cross-sectional area following VAD placement indicating larger muscle fibers. Further, immunohistochemistry using an antibody against fast-twitch, glycolytic myosin showed a high proportion of glycolytic type II muscle fibers in the rectus abdominis muscle samples from patients with advanced HF before VAD placement. Hemodynamic correction following VAD placement decreased the proportion of glycolytic type II fibers with a relative increase of oxidative

type I muscle fibers (type I/type II fiber, 38/62 % pre-VAD versus 54/46 % post-VAD, $p = 0.031$) (Fig. 4b).

Skeletal muscle capillary density analysis did not show significant differences in the number of capillaries per muscle fiber in response to VAD implantation (mean number of capillaries per muscle fiber ratio, 0.34 ± 0.05 pre-VAD versus 0.3 ± 0.06 post-VAD; $p = 0.6$).

Fatty acid oxidation analysis of skeletal muscle tissue from patients before and after VAD implantation showed an increase in the production of [^{14}C] CO_2 from [^{14}C] oleic acid following VAD implantation (+1.37-fold versus pre-VAD; $p = 0.03$) (Fig. 4c). This was accompanied by increased phosphorylation of Akt in skeletal muscle of patients following VAD support compared to pre-VAD implantation (+2.3-fold versus pre-VAD; $p < 0.01$) (Fig. 4d).

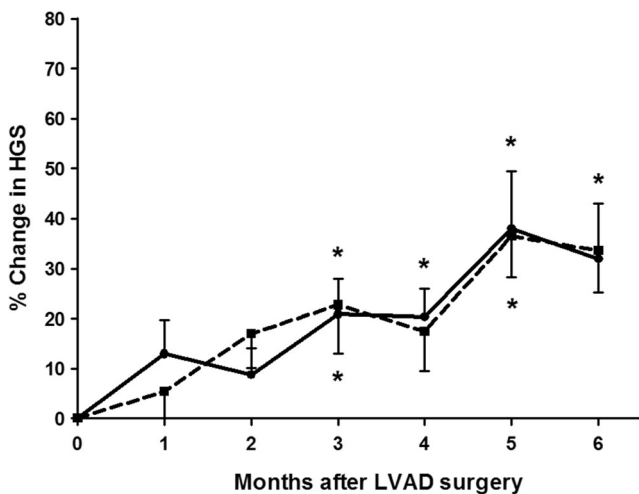


Fig. 2 Functional analysis of skeletal muscle. Hand grip strength improved by around 20 % of baseline pre-VAD values at 90 days following surgery with further increase over the following weeks (* $p < 0.05$ versus baseline, $n = 15$ patients at baseline, solid line—dominant hand, dashed line—non-dominant hand)

3 Discussion

In our current study, we demonstrate that patients with advanced HF develop GH resistance characterized by elevated circulating GH and reduced IGF-1 levels. Following mechanical unloading of the failing myocardium and subsequent hemodynamic normalization, improvement of GH resistance was found accompanied by enhanced local expression of anabolic IGF-1 in skeletal muscle. Further, VAD implantation increased skeletal muscle fiber CSA and improved skeletal muscle oxidative function. These profound anabolic and oxidative changes are accompanied by improved systemic and

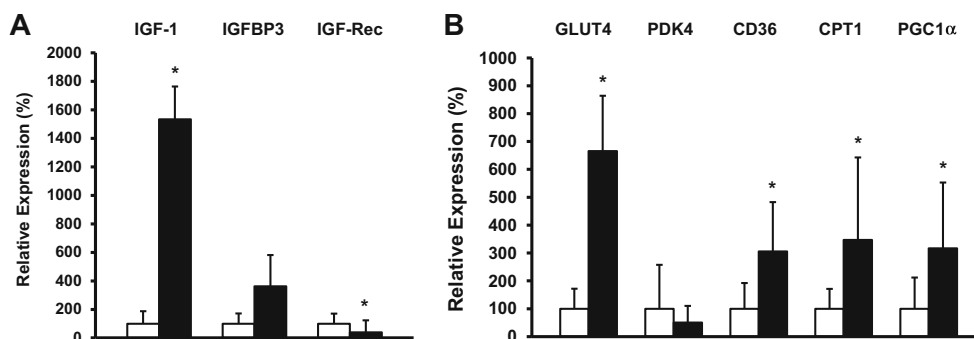


Fig. 3 Analysis of anabolic and metabolic marker gene expression in skeletal muscle before and after VAD implantation. **a** VAD placement results in increased expression of anabolic IGF-1 in skeletal muscle. IGFBP3 remained unchanged while levels of IGF-1 receptor decreased. **b** Analysis of markers of glucose and fatty acid uptake and oxidation in skeletal muscle before and after VAD implantation showed increased expression of GLUT4 following VAD with a non-significant decrease

in PDK4. The fatty acid transporter CD36 and the mitochondrial marker of fatty acid uptake, CPT1, both increased as well. Finally, PGC1 α , the master regulator of oxidative metabolism, increased in skeletal muscle following VAD placement indicating overall increased oxidative metabolism ($*p < 0.05$ versus pre-VAD; $n = 6-10$ per group for all measures; gene expression based on normalization to beta-actin; empty bars—pre-VAD, filled bars—post-VAD)

local metabolic function and increased skeletal muscle hand grip strength.

Skeletal muscle metabolism, morphology, and function are the result of a dynamic network of pathways that are known to be deranged in patients with advanced HF [5, 6]. The metabolic phenotype of skeletal muscle is determined by the relative composition of enzymes and contractile protein isoforms of its individual fibers; therefore, any quantifiable fiber plasticity is reflective of underlying molecular metabolic changes [5]. Reduced oxidative capacity of skeletal muscle is associated with decreased type I oxidative fibers, increased glycolytic type II fibers, mitochondrial dysfunction, and induction of muscle atrophy [25]. Reduction of capillary density in HF, poor peripheral perfusion, and impaired nutritional status further contribute to these changes [4, 9]. Of note, glycolytic generation of ATP results in reduced net production of ATP compared to oxidation of glucose and fatty acids in the mitochondria, leading to energy depletion and decreased glycogen content of skeletal muscle in advanced HF [5]. This peripheral skeletal muscle phenotype mimics the known changes in energy metabolism in the failing myocardium.

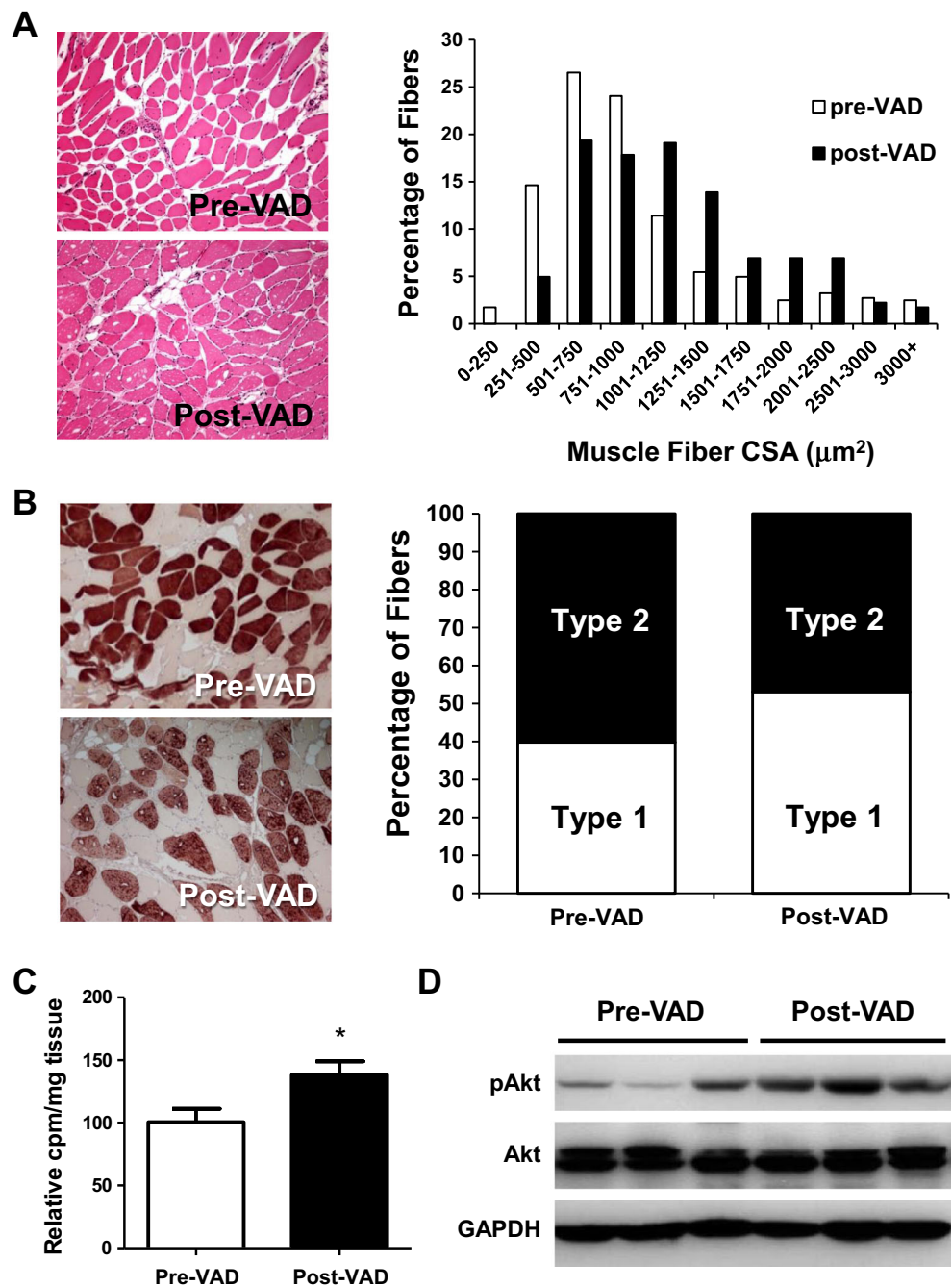
The current study shows a profound effect of VAD implantation on the GH/IGF-1 signaling axis. However, while the GH/IGF-1 ratio improved, the circulating levels of both GH and IGF-1 were not normalized and still showed significant abnormalities compared to controls. The function of this endocrine system is severely deranged in advanced HF with loss of pulsatile GH secretion and development of GH resistance [11], reduced IGF-1 levels [12, 26], and impaired local expression of IGF-1 [12, 24]. Dysfunction of this major anabolic system is known to be associated with loss of body weight, muscle wasting, and impaired survival [10]. Previous trials of GH supplementation in patients with HF have been neutral in outcome or negative [14]. No large clinical trial has evaluated the role of IGF-1 supplementation in HF due to the known

proliferative and neoplastic effects of this molecule which, however, might be overcome by synthetic analogues of regulators and mediators of the GH/IGF-1 axis [10, 27].

The impact of local IGF-1 as a mechanosensitive factor of muscle growth has been studied in various animal models and humans [12, 13, 15, 28]. Muscle denervation, immobilization, and atrophy are all associated with dysfunction of the IGF-1 intracellular signaling cascade [28, 29]. Its molecular result is an induction of ubiquitin-dependent proteolysis, and conversely, overexpression or functional induction of IGF-1 leads to suppression of levels of several ubiquitin E3 ligases [24, 28]. Therefore, IGF-1 and its associated signaling events represent a critical molecular switch mechanism in the balanced regulation of cellular growth and atrophy with profound effects on tissue homeostasis when being dysregulated. Of note, our group has previously shown that both transgenic overexpression of local IGF-1 in skeletal muscle in mice [24] and exercise-induced upregulation of IGF-1 in humans [9] prevent muscle atrophy and impaired metabolism in HF.

Based on our analysis, it is not entirely clear how skeletal muscle oxidative function and local expression of IGF-1 improve following VAD implantation. One hypothesis is that increased mobility of patients with HF following VAD implantation leads to increased muscle activity and, therefore, results from an exercise-like effect on muscle metabolism and structure. On the other hand, improved nutritional status with better absorption of nutrients, increased appetite, and reduced insulin resistance following VAD implantation might affect peripheral skeletal muscle metabolism. Nevertheless, in our cohort, mean BMI did not change significantly following VAD implantation, in contrast to other studies that have reported increases in BMI following VAD implantation in some patients [30]. In a recent study, Emani et al. [31] analyzed BMI characteristics derived from the HeartMate-II clinical trial studies database and describe a significant increase of BMI

Fig. 4 Analysis of skeletal muscle before and after VAD implantation. **a** *Left*, analysis of muscle fiber cross-sectional area on H&E-stained sections of rectus abdominis muscle specimens. Muscle fiber cross-sectional area increased following VAD placement. *Right*, fiber size distribution diagram ($n=6$ samples before and after VAD implantation). **b** VAD implantation is associated with increased number of oxidative type I muscle fibers. *Left*, immunohistochemical analysis of type II myosin (*dark fibers*) reveals a decreased proportion consistent with improved oxidative capacity following VAD placement ($p<0.05$). Oxidative type I fibers are non-stained muscle fibers. *Right*, quantitative analysis of type I versus type II muscle fibers in skeletal muscle before and after VAD implantation ($n=6$ per group; $p=0.04$) **c** VAD implantation results in increased fatty acid oxidation, assessed by increased [^{14}C] CO_2 production in skeletal muscle following VAD placement ($p<0.05$; $n=6$ per group). **d** Increased Akt phosphorylation in skeletal muscle post-VAD implantation ($n=6$ per group; $p=0.012$ versus pre-VAD)



in patients during VAD support, mainly in underweight patients. Our study was not able to reproduce this finding, which might be owed to the considerably smaller number of patients included in our study and differences in baseline BMI before VAD implantation. In the comparable group of the study of Emani et al., in the category “normal” BMI (18.5–29.9 kg/m²), the mean BMI was 24±3 kg/m² while in our study, the mean BMI was 26.8±4.3. Emani et al. reported a small although significant increase of BMI of less than 5 % at 6 months after VAD implantation. However, in the cohort assigned to the “obese” category (mean BMI 32±1 kg/m²),

no significant difference of BMI could be observed at 6 and 24 months after VAD implantation. Furthermore, only 9 % of the patients originally included in the study were analyzed for BMI changes at the 24-month time point which raises the concern of survivor bias in that analysis. Finally, improved peripheral circulation, increased tissue perfusion, and reduced hypoxia both at rest and during exercise appear to contribute to the increased oxidative metabolism in skeletal muscle. Our current study, however, did not show a significant difference in capillary density in skeletal muscle during VAD implantation. Several studies have shown the induction of glycolytic

metabolism at the cost of oxidative ATP generation in the setting of hypoxia in various tissues. The underlying mechanism seems to be a molecular cross talk between an induction of hypoxia-induced factor (HIF)-1 α and reduced expression and activity of the master regulator of oxidative metabolism, PGC-1 α [32]. Consistently, VAD support increased skeletal muscle PGC-1 α levels.

Metabolic marker genes and their expression levels are indicative of the distinct metabolic phenotype of skeletal muscle. Induction in GLUT4 following VAD implantation suggests increased insulin-regulated glucose transport capacity within myocytes. Increased expression of CD36, the fatty acids transporter, and CPT-1, the rate-limiting transporter controlling fatty acid uptake to mitochondria, in skeletal muscle after VAD implantation implies improved fatty acid uptake and oxidation. These changes are consistent with an increased oxidative capacity and increased lipid oxidation rate of skeletal muscle following VAD implantation. Of note, a negative feedback loop seems to involve the expression of the IGF-1 receptor where increased levels of circulating and local IGF-1 are associated with decreased expression of IGF-1 receptor in skeletal muscle following VAD implantation. Nevertheless, increased phosphorylation of Akt in skeletal muscle following VAD implantation indicates increased PI3kinase/Akt signaling downstream of the IGF-1 receptor.

Therapeutic interventions to affect skeletal muscle dysfunction in HF are very limited. No medical therapy targeting muscle dysfunction or metabolism in HF has been established so far, and only exercise training has been consistently linked to improved peripheral muscle metabolism, structure, and function [4]. Exercise training also leads to increased exercise capacity and improved quality of life in patients with HF [9, 11, 12]. Of note, several studies have shown increased oxidative capacity, improved mitochondrial function, reduction in fiber atrophy, as well as increased expression of IGF-1 following exercise training in patients and animal models of HF [4].

Our study is limited by the small sample size and the smaller size of cohorts analyzed in the subsets for histologic and molecular measurements due to tissue collection variability. Therefore, the analysis power of these subsets is smaller than the larger complete cohort.

In conclusion, our data demonstrate that mechanical unloading of the failing myocardium with hemodynamic improvement after VAD implantation leads to correction of GH resistance and increased local levels of IGF-1 in patients with advanced HF. Further, muscle function, oxidative capacity, and ultrastructure improve after VAD implantation. These findings demonstrate that VAD support is associated with a partial correction of metabolic and functional abnormalities of skeletal muscle and impaired GH/IGF-1 signaling in patients with advanced HF.

Acknowledgments This work was supported by grants from the National Heart, Lung and Blood Institute (K23 HL095742-01, P30 HL101272-01, UL1 RR 024156, HL073029, and HL45095) and the Herbert and Florence Irving Scholar Award to Dr. Schulze. Aalap Chokshi was supported by the Doris Duke Fellowship Program. The authors of this manuscript certify that they comply with the ethical guidelines for authorship and publishing in the *Journal of Cachexia, Sarcopenia, and Muscle* [33].

Conflict of interest Tuba Khawaja, MD, Ruiping Ji, MD, Tomoko S. Kato, MD, Katherine Xu, BS, Cynthia Zizola, PhD, Christina Wu, MS, Daniel E. Forman, MD, Takeyoshi Ota, MD, Peter Kennel, MD, Hiroo Takayama, MD, Yoshifumi Naka, MD, PhD, Isaac George, MD, and Donna Mancini, MD declare that they have no conflict of interest.

References

1. Anker SD, Chua TP, Ponikowski P, Harrington D, Swan JW, Kox WJ, et al. Hormonal changes and catabolic/anabolic imbalance in chronic heart failure and their importance for cardiac cachexia. *Circulation*. 1997;96:526–34.
2. Schulze PC, Kratzsch J, Linke A, Schoene N, Adams V, Gielen S, et al. Elevated serum levels of leptin and soluble leptin receptor in patients with advanced chronic heart failure. *Eur J Heart Fail*. 2003;5(1):33–40.
3. Schulze PC, Biolo A, Gopal D, Shahzad K, Balog J, Fish M, et al. Dynamics in insulin resistance and plasma levels of adipokines in patients with acute decompensated and chronic stable heart failure. *J Card Fail*. 2011;17(12):1004–11.
4. Duscha BD, Schulze PC, Robbins JL, Forman DE. Implications of chronic heart failure on peripheral vasculature and skeletal muscle before and after exercise training. *Heart Fail Rev*. 2008;13(1):21–37.
5. Drexler H, Riede U, Munzel T, König H, Funke E, Just H. Alterations of skeletal muscle in chronic heart failure. *Circulation*. 1992;85(5):1751–9.
6. Habedank D, Meyer FJ, Hetzer R, Anker SD, Ewert R. Relation of respiratory muscle strength, cachexia and survival in severe chronic heart failure. *J Cachexia Sarcopenia Muscle*. 2013;4(4):277–85.
7. Tsutsui H, Ide T, Hayashidani S, Suematsu N, Shiomi T, Wen J, et al. Enhanced generation of reactive oxygen species in the limb skeletal muscles from a murine infarct model of heart failure. *Circulation*. 2001;104(2):134–6.
8. Simonini A, Chang K, Yue P, Long CS, Massie BM. Expression of skeletal muscle sarcoplasmic reticulum calcium-ATPase is reduced in rats with postinfarction heart failure. *Heart*. 1999;81(3):303–7.
9. Duscha BD, Kraus WE, Keteyian SJ, Sullivan MJ, Green HJ, Schachat FH, et al. Capillary density of skeletal muscle: a contributing mechanism for exercise intolerance in class II-III chronic heart failure independent of other peripheral alterations. *J Am Coll Cardiol*. 1999;33(7):1956–63.
10. Junnila RK, List EO, Berryman DE, Murrey JW, Kopchick JJ. The GH/IGF-1 axis in ageing and longevity. *Nat Rev Endocrinol*. 2013;9(6):366–76.
11. Anker SD, Volterrani M, Pflaum CD, Strasburger CJ, Osterziel KJ, Doehner W, et al. Acquired growth hormone resistance in patients with chronic heart failure: implications for therapy with growth hormone. *J Am Coll Cardiol*. 2001;38(2):443–52.
12. Hambrecht R, Schulze PC, Gielen S, Linke A, Mobius-Winkler S, Yu J, et al. Reduction of insulin-like growth factor-I expression in the skeletal muscle of noncachectic patients with chronic heart failure. *J Am Coll Cardiol*. 2002;39(7):1175–81.

13. Song YH, Li Y, Du J, Mitch WE, Rosenthal N, Delafontaine P. Muscle-specific expression of IGF-1 blocks angiotensin II-induced skeletal muscle wasting. *J Clin Invest*. 2005;115(2):451–8.
14. Osterziel KJ, Strohm O, Schuler J, Friedrich M, Hanlein D, Willenbrock R, et al. Randomised, double-blind, placebo-controlled trial of human recombinant growth hormone in patients with chronic heart failure due to dilated cardiomyopathy. *Lancet*. 1998;351(9111):1233–7.
15. Hambrecht R, Schulze PC, Gielen S, Linke A, Mobius-Winkler S, Erbs S, et al. Effects of exercise training on insulin-like growth factor-I expression in the skeletal muscle of non-cachectic patients with chronic heart failure. *Eur J Cardiovasc Prev Rehab*. 2005;12(4):401–6.
16. Lund LH, Freda P, Williams JJ, LaManca JJ, LeJemtel TH, Mancini DM. Growth hormone resistance in severe heart failure resolves after cardiac transplantation. *Eur J Heart Fail*. 2009;11(5):525–8.
17. Miller LW, Pagani FD, Russell SD, John R, Boyle AJ, Aaronson KD, et al. Use of a continuous-flow device in patients awaiting heart transplantation. *N Engl J Med*. 2007;357(9):885–96.
18. Park SJ, Milano CA, Tatoes AJ, Rogers JG, Adamson RM, Steidley DE, et al. Outcomes in advanced heart failure patients with left ventricular assist devices for destination therapy. *Circ Heart Fail*. 2012;5(2):241–8.
19. Kato TS, Chokshi A, Singh P, Khawaja T, Cheema F, Akashi H, et al. Effects of continuous-flow versus pulsatile-flow left ventricular assist devices on myocardial unloading and remodeling. *Circ Heart Fail*. 2011;4(5):546–53.
20. Kato TS, Chokshi A, Singh P, Khawaja T, Iwata S, Homma S, et al. Markers of extracellular matrix turnover and the development of right ventricular failure after ventricular assist device implantation in patients with advanced heart failure. *J Heart Lung Transplant*. 2012;31(1):37–45.
21. Khan RS, Kato TS, Chokshi A, Chew M, Yu S, Wu C, et al. Adipose tissue inflammation and adiponectin resistance in patients with advanced heart failure: correction after ventricular assist device implantation. *Circ Heart Fail*. 2012;5(3):340–8.
22. Mancini D, Goldsmith R, Levin H, Beniaminovitz A, Rose E, Catanese K, et al. Comparison of exercise performance in patients with chronic severe heart failure versus left ventricular assist devices. *Circulation*. 1998;98(12):1178–83.
23. Chokshi A, Drosatos K, Cheema FH, Ji R, Khawaja T, Yu S, et al. Ventricular assist device implantation corrects myocardial lipotoxicity, reverses insulin resistance, and normalizes cardiac metabolism in patients with advanced heart failure. *Circulation*. 2012;125(23):2844–53.
24. Schulze PC, Fang J, Kassik KA, Gannon J, Cupesi M, MacGillivray C, et al. Transgenic overexpression of locally acting insulin-like growth factor-1 inhibits ubiquitin-mediated muscle atrophy in chronic left-ventricular dysfunction. *Circ Res*. 2005;97(5):418–26.
25. Zierath JR, Hawley JA. Skeletal muscle fiber type: influence on contractile and metabolic properties. *PLoS Biol*. 2004;2(10):e348.
26. Niebauer J, Pflaum CD, Clark AL, Strasburger CJ, Hooper J, Poole-Wilson PA, et al. Deficient insulin-like growth factor I in chronic heart failure predicts altered body composition, anabolic deficiency, cytokine and neurohormonal activation. *JACC*. 1998;32(2):393–7.
27. Lenk K, Palus S, Schur R, Datta R, Dong J, Culler MD, et al. Effect of ghrelin and its analogues, BIM-28131 and BIM-28125, on the expression of myostatin in a rat heart failure model. *J Cachexia Sarcopenia Muscle*. 2013;4(1):63–9.
28. Stitt TN, Drujan D, Clarke BA, Panaro F, Timofeyeva Y, Kline WO, et al. The IGF-1/PI3K/Akt pathway prevents expression of muscle atrophy-induced ubiquitin ligases by inhibiting FOXO transcription factors. *Mol Cell*. 2004;14(3):395–403.
29. Bodine SC, Stitt TN, Gonzalez M, Kline WO, Stover GL, Bauerlein R, et al. Akt/mTOR pathway is a crucial regulator of skeletal muscle hypertrophy and can prevent muscle atrophy in vivo. *Nat Cell Biol*. 2001;3(11):1014–9.
30. Raymond AL, Kfoury AG, Bishop CJ, Davis ES, Goebel KM, Stoker S, et al. Obesity and left ventricular assist device driveline exit site infection. *ASAIO J*. 2010;56(1):57–60.
31. Emani S, Brewer RJ, John R, Slaughter MS, et al. Patients with low compared with high body mass index gain more weight after implantation of a continuous-flow left ventricular assist device. *J Heart Lung Transplant*. 2013;32:31–5.
32. Tadaishi M, Miura S, Kai Y, Kano Y, Oishi Y, Ezaki O. Skeletal muscle-specific expression of PGC-1 α -b, an exercise-responsive isoform, increases exercise capacity and peak oxygen uptake. *PLoS One*. 2011;6(12):e28290.
33. von Haehling S, Morley JE, Coats AJ, Anker SD. Ethical guidelines for authorship and publishing in the *Journal of Cachexia, Sarcopenia, and Muscle*. *J Cachexia Sarcopenia Muscle*. 2010;1:7–8.